Microfluid Nanofluid (2008) 4:343–348
DOI 10.1007/s10404-007-0184-1

SHORT COMMUNICATION

Microfluidic sorting of droplets by size

Yung-Chieh Tan · Yao Li Ho · Abraham Phillip Lee

Received: 23 March 2007 / Accepted: 21 May 2007 / Published online: 29 June 2007

Abstract Droplet sorting by size was achieved in microfluidic channels through controlling the bifurcating junction geometry and the flow rates of the daughter channels. The sorting designs separated droplets with a radius difference of as little as 4 μm. The developed droplet channel design can be potentially used in combination with other particle sorting system to improve the sorting efficiency without the control of electrodes or fluidic valves.

Keywords Sorting · Droplets · Size

1 Introduction

Droplet microfludics is a rapidly growing field that has numerous applications in biology, medicine, and chemistry. Examples of currently applicable technology include droplet based on-chip system for PCR (Guttenberg et al. 2004), protein crystallization (Zheng et al. 2003), chemical mixing (Chabert et al. 2005; Kohler et al. 2004; Tan et al. 2004, 2006a, b, c), nanoparticle synthesis (Hung et al. 2006), cell encapsulation (He et al. 2005 and Tan et al. 2006b), and vesicle generation (Tan et al. 2006b). As a result many fundamental techniques in droplet control had been developed. For example, the droplet size and the generation frequency can be controlled by varying the flow rates of the immiscible flows (Thorsen et al. 2001; Anna et al. 2003; Tan et al. 2006a). The droplet volume may further be splitted (Tan et al. 2004; Link et al. 2004) into two daughter droplets or fused with additional droplets (Kohler et al. 2004; Tan et al. 2004, 2006c) through the control of channel geometry. Yet, there has been no report of a passive microfluidic sorting system that is capable of separating droplets that are only micrometers difference in size. Here we demonstrate a new size sorting mechanism that causes droplets to sort into two different daughter channels under a fixed flow rate. The droplet sorting is achieved through controlling the channel geometry and the flow rates of the daughter channels.

Y.-C. Tan · Y. L. Ho · A. P. Lee (✉)
Department of Biomedical Engineering,
University of California Irvine, Irvine,
California, USA
e-mail: aplee@uci.edu

2 Principle

In our system, droplets are sorted at a bifurcating junction. The bifurcating junction divides the flow carrying the droplet into two daughter flows. Each daughter flow exerts a shear force on the droplet. The difference in the shear forces experienced by the droplet causes it to move in the direction of the higher daughter flow. The shear forces experienced by the droplet depend on both the ratio of the areas projected by the daughter flows and the ratio of the shear rates generated by the daughter flows. According to the variables shown in Fig. 1, we define the flow rate ratio as (Qz/Qv), such that Qz is the flow rate of the daughter channel Z and Qv is the flow rate of the daughter channel V. Since shear rate is proportional to the flow rate and inversely proportional to the square of channel width, the resulting shear rate ratio is (Qz/Qv) $(Wv/Wz)^2$. The area projected by the daughter flows vary with both (Qz/Qv) and the size of the droplets. As illustrated in Fig. 1c, a higher daughter flow (Z) affects a much larger droplet area than a lower daughter flow (V). From the variables of Fig. 1b, we can establish the following expression for the projected area ratio (PAR) by the daughter flows:

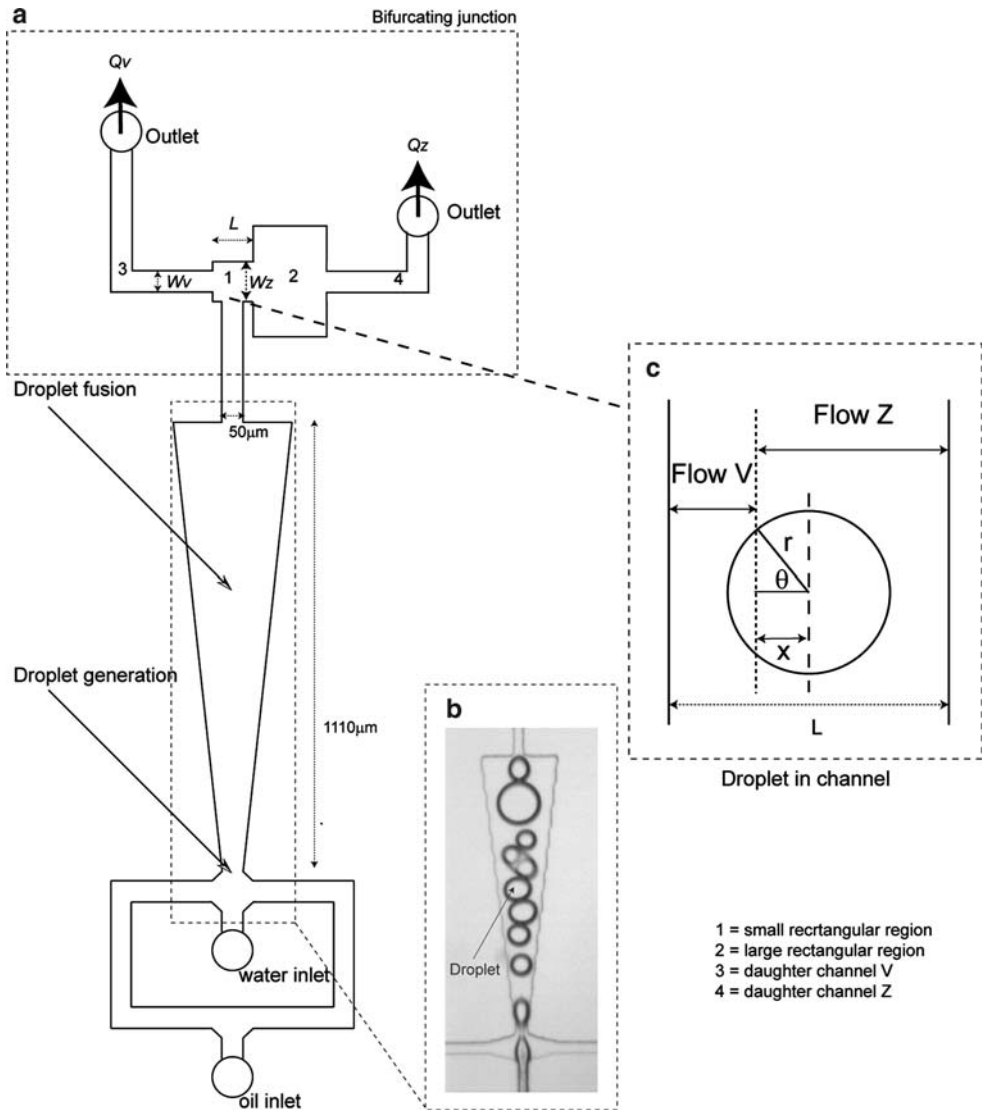

Fig. 1 **a** The channel schematics showing the general features of the design. From the bottom up droplets were first generated by shear viscous interaction of water and oil. Then the droplets traveled up into the channel expansion where some droplets fused into larger droplets. The droplets eventually flew into the bifurcating junction where droplets were sorted into the daughter channels. The sorting junction consists of two interconnected rectangular regions. The small rectangular region connects to daughter channel *V* and the large rectangular region connects to daughter channel *Z*. The three types of junctions used to sort droplets are shown in Figs. 2a, 3a, and 4a. The lengths of daughter channel *V* is longer than the length of daughter channel *Z*, which caused *Qz* to be greater than *Qv*. **b** Light microscopy image of droplet fusion. (C) Schematic showing the distribution of the daughter flows (flow *V* and flow *Z*) on a droplet. Since *Qz* is greater than *Qv*, the area projected by flow *Z* is always greater than the area projected by flow *V*. The variables used to derive the shear force ratios are indicated in the figure. *r* is the radius of the droplet, *x* is the horizontal distance from the center of the droplet to the dividing point of flow *Z* and flow *V*, and θ is the angle between *r* and *x*

$$((180-\theta)\pi r^2/180+x^2\tan\theta)/(\pi r^2-((180-\theta)(\pi r^2/180)+x^2\tan\theta))).$$

The variable *x* is the horizontal distance from the center of the droplet to the dividing point of flow *Z* and flow *V*. The variable *x* has the expression of

$x = ((Qz/Qv)/(1 + (Qz/Qv))–0.5)\ L$, where *L* is the length of the small rectangular region in the bifurcating junction.

The shear force ratio equals to the product of shear rate ratio and the projected area ratio. For any droplets in the microfluidic channel, a shear force ratio of greater than 1 indicates that it should sort into daughter channel *V*, and a

value of less than 1 indicates that it should sort into daughter channel *Z*.

3 Materials and methods

We made the microfluidic channels by plasma bonding SU-8 patterned PDMS channels to clean glass slides (McDonald and Duffy 2000). We controlled the liquid flows by using two syringe pumps (*Pico Plus*, Harvard Apparatus) and recorded the droplet sorting processes using a high speed camera (Fastcam PCI-10K, Photron Ltd). The channel schematics shown in Fig. 1a illustrate the experimental design. Starting from the bottom of the channel, DI water flew into the channel from the middle inlet while oleic acid (viscosity of 27.64 mPa and interfacial tension of 15.6 dyn cm^{-1}) flew in from the bottom inlet. The water flow rate used in the experiments ranged from 0.1 to 0.5 μL min^{-1}, and the oleic acid flow rate used in the experiments ranged from 0.2 to 5 μL min^{-1}. Downstream from the droplet generation point, the expanding trapezoid channel decreased the velocity of the flow, thus allowing some droplets to fuse into larger droplets. This fusion created a distribution of large and small droplets that eventually flew into the bifurcating junction.

We designed three different types of channels to test the sorting of droplets. The channel designs were identical in all parts excepting the geometry of the bifurcating junction. The geometry of the three bifurcating junction designs, $\Sigma\alpha$, $\Sigma\beta$, and $\Sigma\psi$, are detailed in Figs. 2a, 3a, and 4a, respectively. In all types of channel junctions, we designed the length of daughter channel *V* to be shorter than the length of daughter channel *Z* to allow the flow rate of daughter channel *Z* to be greater than the flow rate of daughter channel *V*. We tested droplet sorting in each type of channel design using four sets of channel lengths. These channel lengths provided calculated flow rate ratios (Qz/Qv) of 1.25, 1.5, 2.5, and 4.5.

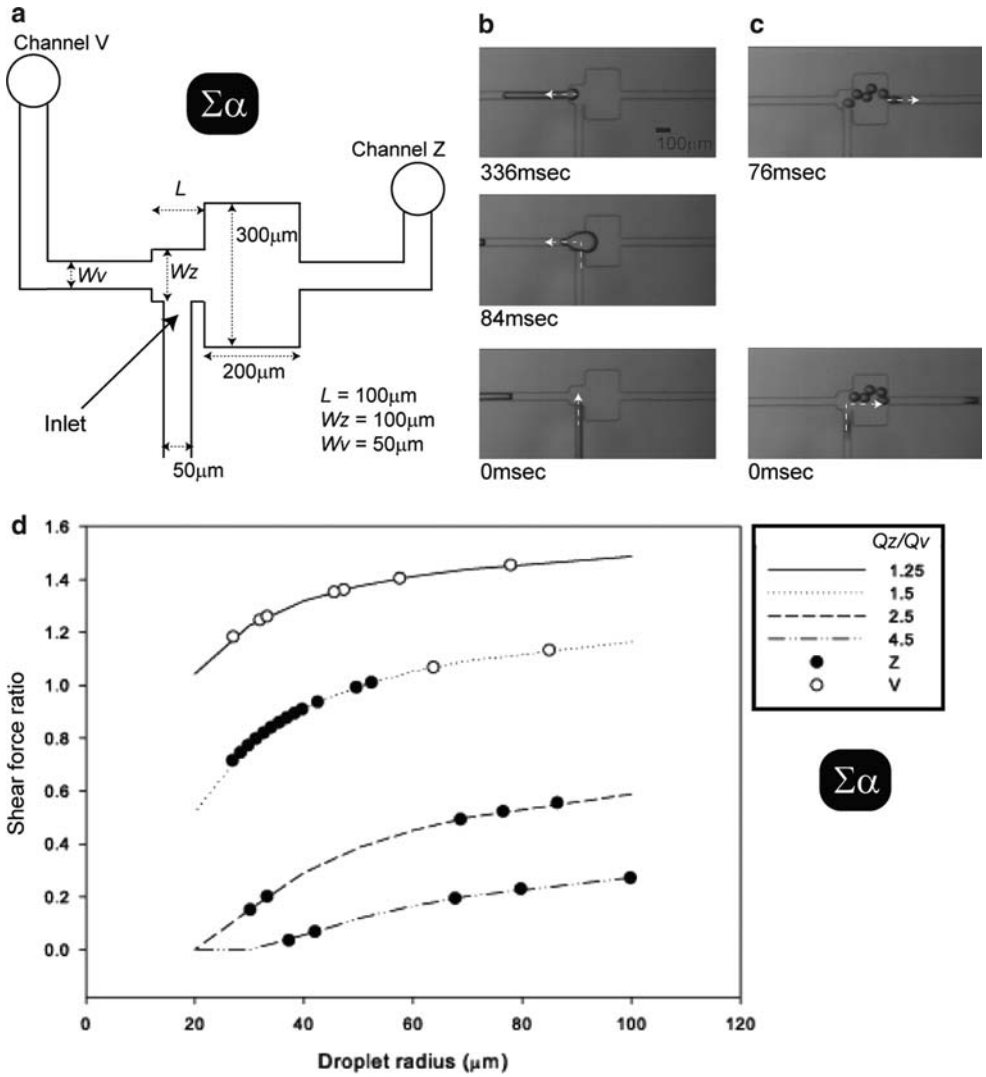

Fig. 2 **a** Schematic of junction design $\Sigma\alpha$. The *arrow* indicates the inlet that allowed droplets to be position into the center of the small rectangular region. **b**, **c** The sorting of droplets by size in channel $\Sigma\alpha$ design. **b** Large droplets were sorted into channel *V*,and **c** small droplets were sorted into channel *Z*. **d** The distribution of sorted and unsorted droplet sizes varied with the flow rate ratio. The shear force ratio accurately indicated droplet sorting such that all the droplets that were sorted into daughter channel *V* occurred at a shear force ratio of greater than 1, and all droplets that were sorted into daughter channel *Z* occurred at a shear force ratio of less than 1

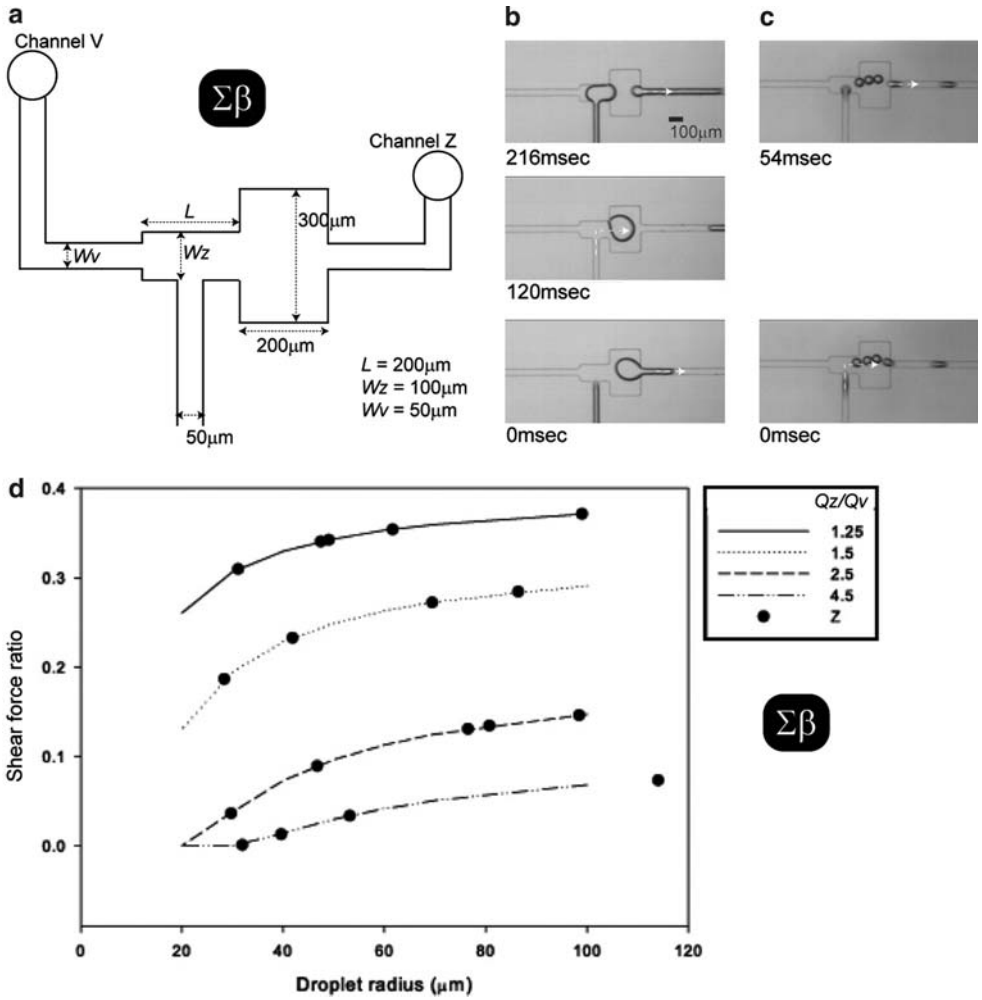

Fig. 3 **a** Schematic of junction design $\Sigma\beta$. In contrast to $\Sigma\alpha$ design, the length of the small rectangular region is extended to be 200 μm. **b** The increased length of the small rectangular region prevented droplet sorting by size. Both large droplets and **c** small droplets were all sorted into daughter channel *Z*. **d** The calculated shear force ratio showed the sorting of droplets in the $\Sigma\beta$ channel designs all occurred at a shear force ratio of less than 1, which indicated that no droplet sorting can occur in $\Sigma\beta$ channel designs

In a channel with symmetric bifurcating junction geometry, the tested *Qz/Qv* ratios would cause all droplets to sort into the daughter channel *Z*. However, we designed the bifurcating junction geometry to compensate the sorting effect caused by the flow rate difference between the daughter channels. The three bifurcating junction designs shown in Figs. 2a, 3a, and 4a have similar geometry showing two interconnected rectangular regions. In all three designs, the large rectangular region is directly connected to daughter channel *Z* and the smaller region is directly connected to daughter channel *V*. Since the local shear rate in the channel is inversely proportional to the square of the channel width, the larger rectangular region would reduce the magnitude of the local shear force exerted by *Qz* on the droplets. At the same time, the smaller rectangular region would increase the magnitude of the local shear force exerted by *Qv* on the droplets. Thus, the effect of the bifurcating junction geometry favors the flow of droplets into daughter channel *V* while the effect of the difference in flow rates between the two daughter channels favors the flow of droplets into daughter channel *Z*. We used all three types of channels to investigate the combination of the effect of the junction geometry and the difference in the flow rates of the daughter channel. The tested droplet sizes ranged from 20 to 100 μm.

4 Results

Fig. 2b and c show the droplet sorting results of $\Sigma\alpha$ channel design. Large droplets were sorted into the daughter channel *V* and small droplets were sorted into daughter channel *Z*. Figure 2d shows the relationship between the calculated shear force ratio and the sorting of the droplets. The droplet sizes showing in Fig. 2d was measured from the experiments. As indicated by the flow rate ratios in Fig. 2d, the size of droplets sorted into daughter channel *V* increased when we increased the flow rate ratio. When the flow rate ratio (*Qz/Qv*) was equal to 1.25, the effect of bifurcating junction geometry was stronger than the effects of the flows, causing droplets of all sizes to sort into the daughter channel *V*. However, when the flow rate ratio was

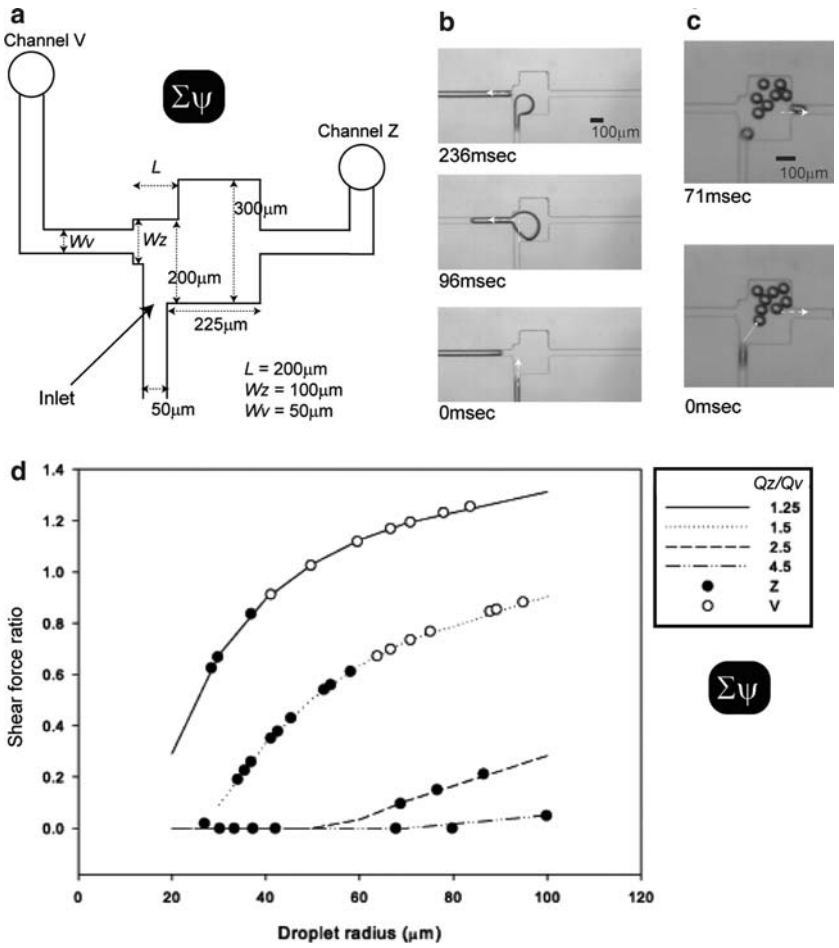

Fig. 4 **a** Schematic of junction design $\Sigma\psi$. Similar to junction design $\Sigma\alpha$ but the inlet (indicated by the *arrow*) joins the large rectangular region prior to reaching the small rectangular region. This difference caused droplets to shift to the intersection between the large and small rectangular region prior to sorting. This shifting effect favored the sorting of droplets into daughter channel *Z*. **b** Sorting of large droplets. **c** Sorting of small droplets. **d** The shear force ratio was calculated based on a fixed channel geometry, which did not account for the shifting in the position of droplets prior to sorting. Thus the shear force ratio did not indicate the sorting of droplets. Nevertheless, the distribution of sorted and unsorted droplets showed that junction design $\Sigma\psi$ can sort droplets at a lower flow ratio than junction design $\Sigma\alpha$

equal to 1.5, droplets sorted into different channels according to their sizes. When the flow ratio was equal to 1.5, the calculated shear force ratio indicated that the critical droplet sorting radius is ~50 μm. This corroborates with the experimental results that droplets with radii larger than 64 μm were sorted into daughter channel *V* while droplets with radii smaller than 50 μm were sorted into daughter channel *Z*. The difference in the radius of these two droplet sizes indicated that the sorting precision is at least 14 μm. Although the precision may be smaller than 14 μm, it is not measurable in the current setup. Droplets of all sizes sorted into the daughter channel *Z* when the flow rate ratio was increased to 2.5 and 4.5.

Unlike the $\Sigma\alpha$ channel design, the $\Sigma\beta$ design did not produce droplet sorting by size at any of the tested flow ratios. Fig. 3b and c show that all of the tested droplets sorted into daughter channel *Z*. The difference in droplet sorting between $\Sigma\alpha$ channel design and $\Sigma\beta$ channel design was created by the increased length of the small rectangular region. The length of the small rectangular region in $\Sigma\beta$ channel design is twice the length of the small rectangular region in $\Sigma\alpha$ channel design. The increased length of the small rectangular region positioned droplets far away from experiencing the difference in the shear forces caused by the channel geometry. The calculated shear force ratios accurately indicated that no droplets can be sorted in $\Sigma\beta$ type channels. As shown in Fig. 3d, the shear force ratios calculated from the droplet sizes are all below 1, indicating that all the droplets would flow into daughter channel *Z*.

In the $\Sigma\psi$ channel design, droplets were also sorted according to their sizes as shown by Fig. 4b, c. In contrast to channel design $\Sigma\alpha$, channel design $\Sigma\psi$ is able to produce droplet sorting starting at a lower flow ratio. The sorting of droplets in $\Sigma\psi$ channel design occurred at flow rate ratios of 1.25 and 1.5. This difference in sorting was caused by joining the inlet (Fig. 4a) directly to the large rectangular region. Such modifications in the channel design caused droplets to be positioned near the intersection (between the small rectangular region and the large rectangular region) prior to sorting. In contrast, the droplet was positioned in the center of the small rectangular region prior to sorting in the $\Sigma\alpha$ channel design (Fig. 2a). This shifting of droplet positions in channel design $\Sigma\psi$ caused the droplets to shift toward regions of higher flow rate prior to sorting. The position difference of the droplets at the bifurcating junction thus favored the sorting of droplets into daughter

channel *Z*. At a flow ratio of 1.25, droplets with radii smaller than 37 μm were sorted into daughter channel *Z* and droplets with radii larger than 41 μm were sorted into daughter channel *V*. The difference in the radius of the two droplet sizes indicated that the sorting precision was at least 4 μm at the flow ratio of 1.25. When we increased the flow rate ratio to 1.5, droplets with radii smaller than 58 μm were sorted into daughter channel *Z* and droplets with radii larger than 64 μm were sorted into daughter channel *V*. The difference in the radii of the two droplet sizes indicated that the sorting precision was at least 6 μm at the flow ratio of 1.5. The calculated shear force ratios also showed enhanced sorting effects caused by the shifting in the positions of the droplets at the bifurcating junction. While the sorting of droplets into daughter channel *V* occurred at a shear force ratio of 0.91, it does not contradict the prediction that droplets are sorted into daughter channel *V* when the shear force ratio is greater than 1. Calculated from $Wv = 50$ μm and $Wz = 100$ μm, the shear force ratio was based on a fixed channel geometry, and it did not account for the position change caused by the difference in daughter flows prior to droplet sorting. Since the shifting in the position of droplets favors the sorting of droplets into daughter channel *Z*, the actual shear force ratio should be higher than the calculated values. In addition, the actual shear force ratio would vary with the size of the droplets because the shifting in the position of droplets would also vary with their sizes. These effects are too complex to be determined by the geometry of the channel alone. Nevertheless, the $\Sigma\psi$ channel design, in comparison with the $\Sigma\alpha$ channel design, clearly showed that a lower flow rate ratio can be used to produce the droplet sorting phenomenon.

5 Conclusion

We have demonstrated the sorting of droplets by size through testing three bifurcating channel geometries. The experimental results indicated that droplets can be sorted into different daughter channels according to their sizes by simultaneously controlling the flow rate ratio of the daughter channels and the bifurcating junction geometry. Droplet sorting was observed in the $\Sigma\alpha$ channel design and in the $\Sigma\psi$ channel design, but not in the $\Sigma\beta$ channel design. The calculated shear force ratios accurately indicated the sorting potential of the $\Sigma\alpha$ channel design and the $\Sigma\beta$ channel design, but failed to determine sorting for the $\Sigma\psi$ channel design. The designs and the sorting principle presented here may aid in the development of particle filtration systems and droplet sorting microfluidic chips.

References

Anna SL, Bontoux N, Stone HA (2003) Formation of dispersions using "flow-focusing" in microchannels. Appl Phys Lett 82:364–366

Chabert M, Dorfman KD, Viovy JL (2005) Droplet fusion by alternating current (AC) field electrocoalescence in microchannels. Electrophoresis 26:3706–3715

Guttenberg Z, Müller H, Habermüller H, Geisbauer A, Pipper J, Felbel J, Kielpinski M, Scriba J, Wixforth A (2004) Planar chip device for PCR and hybridization with surface acoustic wave pump. Lab Chip 5:308–317

He M, Edgar JS, Jeffries GDM, Lorenz RM, Shelby JP, Chiu DT (2005) Selective encapsulation of single cells and subcellular organelles into picoliter- and femtoliter-volume droplets. Anal Chem 77:1539–1544

Hung LH, Choi KM, Tseng WY, Tan YC, Shea KJ, Lee AP (2006) Alternating droplet generation and controlled dynamic droplet fusion in microfluidic device for CdS nanoparticles synthesis. Lab Chip 6:174–178

Kohler JM, Henkel T, Grodrian A, Kirner T, Roth M, Martin K, Metze J (2004) Digital reaction technology by micro segmented flow-components, concepts and applications. Chem Eng J 101:201–216

Link DR, Anna SL, Weitz DA, Stone HA (2004) Geometrically mediated breakup of drops in microfluidic devices. Phys Rev Lett 92:05403–05404

McDonald JC, Duffy DC (2000) Fabrication of microfluidic systems in poly(dimethylsiloxane). Electrophoresis 21:27–40

Tan YC, Fisher JS, Lee AI, Cristini V, Lee AP (2004) Design of microfluidic channel geometries for the control of droplet volume, chemical concentration, and sorting. Lab Chip 4:292–298

Tan YC, Cristini V, Lee AP (2006a) Monodispersed microfluidic droplet generation by shear focusing microfluidic device. Sens Actuator B 114:350–356

Tan YC, Hettiarachchi K, Siu M, Pan YR, Lee AP (2006b) Controlled microfluidic encapsulation of cells, proteins and microbeads in lipid vesicles. JACS 128:5656–5658

Tan YC, Ho YL, Lee AP (2006c) Droplet coalescence by geometrically mediated flow in microfluidic channels. Microfluidics Nanofluidics 10.1007/s10404–006-0136-1

Thorsen T, Roberts RW, Arnold FH, Quake SR (2001) Dynamic pattern formation in a vesicle-generating microfluidic device. Phys Rev Lett 86:4163–4166

Zheng B, Roach LS, Ismagilov (2003) RF, screening of protein crystallization conditions on a microfluidic chip using nanoliter-size droplets. J Am Chem Soc 125:11170–11171